Port-Hamiltonian Modelling of Modular Multilevel Converters with Fixed Equilibrium Point

Gilbert Bergna-Diaz, Santiago Sanchez and Elisabetta Tedeschi
Norwegian University of Science and Technology
Department of Electric Power Engineering,
O. S. Bragstads plass 2E, Trondheim, Norway
Emails: {gilbert.bergna, santiago.sanchez, elisabetta.tedeschi}@ntnu.no

***Abstract*—The paper presents the derivation of a port-Hamiltonian model of a steady-state time-invariant averaged modular multilevel converter (MMC). The MMC can not be expressed in a straightforward way in a port-Hamiltonian framework due to the lack of skew-symmetry of its interconnection matrices. This work proposes a change of variable and a new per unit notation to overcome this limitation.**

***Keywords*—Modular Multilevel Converter; Port Hamiltonian Modelling; Variable Change; Steady-State Time-Invariance.**

I. Introduction

The main objective of this paper is to derive a mathematical representation of the Modular Multilevel Converter (MMC) using the generalized Hamiltonian formalism as presented in [1] and [2], following the procedure of application to power electronic converters presented in [3]. The port-Hamiltonian modelling approach is considered a control paradigm, combining the two following main approaches [4]. First, a port-based modelling approach build upon power preserving interconnections (as opposed to more traditional input-output signal processing viewpoint). Second, a Hamiltonian formulation, that emphasizes the geometry of the state space and the Hamiltonian function (total stored energy) as basic concepts for modelling multi-physics systems. From a control perspective, it provides a natural starting point, especially in the nonlinear case where it is widely recognized that physical properties of the system (such as balance and conservation laws and energy considerations) should be exploited and/or respected in the control design [5]. An almost straightforward application of the MMC converter in a port-Hamiltonian framework would be to use the Passivity property [6] to design globally asymptotically stable controllers. In particular, the passivity-based technique presented in [7] for a two-level Voltage Source Converter (2L-VSC) stands out, as it is based on a simple PI controller widely accepted by practitioners. Nonetheless, the application of such theory requires a port-Hamiltonian formulation which is steady-state time-invariant (SSTI) as opposed to time-periodic (SSTP). Therefore, the starting point adopted in this work is not the averaged model of the MMC converter in its natural time-periodic phase coordinates, but the equivalent SSTI averaged formulation, recently presented in [8].

This paper is organized as follows: First, a brief review on MMC models suited for the intended application is given in section II. Second, an attempt to directly formulate the SSTI model of [8] using the port-Hamiltonian formalism is presented in section III, and its limitations are highlighted. Third, a mathematical reformulation of the model of [8] is presented in section IV such that the previous limitations are avoided, resulting in a port-Hamiltonian model for the MMC. Fourth, the port-Hamiltonian representation of the MMC based on the reformulated SSTI model is validated in section V using time-domain simulations with respect to reference models. Finally, conclusions are drawn in section VI.

II. On the Modelling of Modular Multilevel Converters

A. Generalities of the detailed model

The MMC topology under consideration is represented in full-detail in Fig. 1. The converter is formed by three upper arms and three lower arms. In turn, an arm is formed by an arm inductor (represented by its inductance L_σ and resistance R_σ) connected in series with N series-connected sub-modules (SMs) in half bridge configuration, each formed by two IGBTs and their respective free wheeling diode, as well as one capacitor with equivalent capacitance C. In addition, three filter inductors with equivalent inductance L_f and resistance R_f are used to interface the output of the MMC of each phase with the ac voltage at the point of interconnection v_k^G, where the subscript k indicates a generic phase; i.e., $k \in (abc)$. Furthermore, i_k^U and i_k^L are the currents in the upper and lower arms, respectively, whereas i_k^Δ, referred to as

the grid current, is the current flowing through the filter inductor towards the ac grid. Finally, the dc side of the converter under study will be simply represented by a stiff dc source at a constant voltage v_{dc}, and a dc current i_{dc} flowing form the source to the converter.

B. Continuous MMC model with oscillatory state and control variables in steady-state operation

A simplified modelling approach for the MMC useful for control design and system analysis is shown in the lower right part of Fig. (1). This modelling approach, here referred to as the Arm Averaged Model (AAM), is represented by a controlled voltage source (instead of the series connected SMs) and by an equivalent arm capacitance $C_\sigma = C/N$, representing the internal arm voltage dynamics [9], [10], [11]. This simplification does not consider the switching dynamics of the IGBTs nor the dynamics of the sub-module capacitor voltage balancing algorithm, but instead is based on the averaged continuous behaviour of the arm, and still preserves relevant non-linearities of the MMC.

The AAM representation includes explicit representation of the currents and voltages associated with each phase and each arm of the MMC. These variables are time-periodic in steady state operation, with frequency components defined by the grid frequency and its integer multiples [12], [13], [9]. Thus, the AAM representation of the MMC is referred to in this paper as a Steady-State Time-Periodic (SSTP) model. Although the AAM representation of MMCs is very useful for analysis and simulation, this model in its current form is not directly suited for Port-Hamiltonian modelling which requires a uniquely defined equilibrium point for each operating condition, which corresponds to all state variables settling to constant values in steady-state; i.e., a Steady-State Time-Invariant (SSTI) model. For this reason, dynamic state-space models of three-phase electrical systems, including electrical machines and conventional VSCs are commonly represented in a Synchronously Rotating Reference Frame by applying Park's transformation [14], [15]. However, the arm currents and aggregated arm voltages of an MMC can contain multiple frequency components during regular steady-state operation [13], [9]. This intrinsic characteristic of the MMC topology prevent explicit modelling of all relevant dynamics by directly transforming the arm currents and arm voltages into a single SRRF. Thus, structure-preserving state-space modelling of MMC dynamics is a challenge that has only been recently addressed.

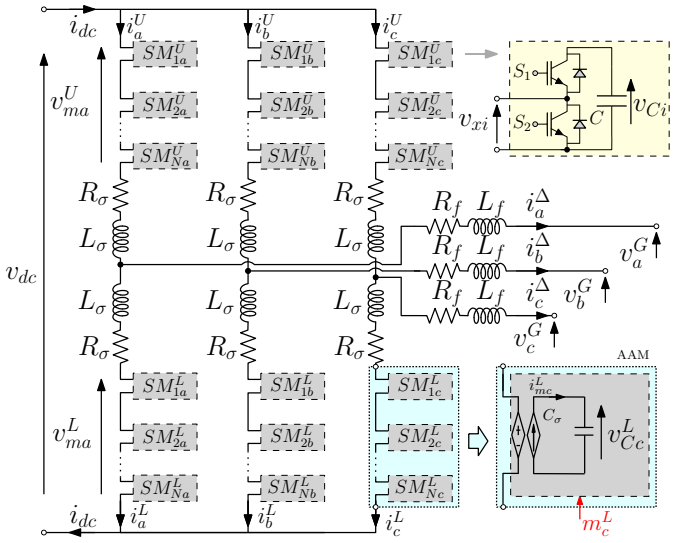

Fig. 1. MMC Topology and AAM for the lower arm (phase C)

C. Continuous MMC model with constant state and control variables in steady-state operation

Modelling approaches able to represent the dynamics the MMC with constant state and control variables in steady-state have recently begun to appear in the literature such as [16], [17], [18], [19], [8]. However, most of these models were aimed at obtaining a SSTI MMC model in order to further linearize it around a well defined equilibrium point, such that small-signal stability analysis could be performed by means of traditional eigenvalue methods [20] common in the power system community. As consequence, the methods used to obtained the SSTI models proposed in [16], [17], [19] are based on linear harmonic superposition, corresponding to phasor-based modelling, which could affect the information about the non-linear characteristics of the MMC, and correspondingly limit the applicability of the models in non-linear techniques for control and analysis. A similar approximation was also made when separately modelling the fundamental frequency and second harmonic frequency dynamics of the the upper and lower arm capacitor voltages in [18]. However, for the model presented in [8], the harmonic superposition was avoided by reformulating the MMC model by representing the internal capacitor voltages and the insertion indexes of the MMC as the sum and difference of the variables corresponding to the upper and lower arms. This approach ensured frequency separation as part of the initial model description, and allowed for transforming all variables into their associated SRRFs without assuming harmonic superposition, resulting in a structure-preserving SSTI model.

Based on the above discussion, the present work is

based on the structure-preserving SSTI MMC model proposed in [8], as it seems to be the most suited model for the Port-Hamiltonian viewpoint. Indeed, the reader is referred to [8] for the complete mathematical proof and validation of this model. However, some of the key features of its derivation are enumerated in the following for convenience.

1) AAM dynamics in Σ-Δ representation: The AAM dynamics, used as a starting point for the derivation of the SSTI model under consideration, can be re-written using a Σ-Δ variable change, representing the sum and difference of the state and control variables corresponding to the upper and lower arms of the converter. This results in the state-space system for a generic phase k in (1), where (1a) represents the dynamics of the voltage sum betwen the arms $v_{Ck}^{\Sigma} = v_{Ck}^{U} + v_{Ck}^{L}$, while (1b) the dynamics of the voltage difference $v_{Ck}^{\Delta} = v_{Ck}^{U} - v_{Ck}^{L}$ between them. In addition, (1c) models the dynamic of the circulating current $i_k^{\Sigma} = (i_k^U + i_k^L)/2$, whereas (1d) represents the dynamics of the grid current $i_k^{\Delta} = i_k^U - i_k^L$.

$$C_\sigma \frac{dv_{Ck}^{\Sigma}}{dt} = m_k^{\Sigma} i_k^{\Sigma} + \frac{1}{2} m_k^{\Delta} i_k^{\Delta}; \tag{1a}$$

$$C_\sigma \frac{dv_{Ck}^{\Delta}}{dt} = m_k^{\Delta} i_k^{\Sigma} + \frac{1}{2} m_k^{\Sigma} i_k^{\Delta}; \tag{1b}$$

$$L_\sigma \frac{di_k^{\Sigma}}{dt} = \frac{v_{dc}}{2} - \frac{\left(m_k^{\Sigma} v_{Ck}^{\Sigma} + m_k^{\Delta} v_{Ck}^{\Delta}\right)}{4} - R_\sigma i_k^{\Sigma} \tag{1c}$$

$$L_\delta \frac{di_k^{\Delta}}{dt} = -v_k^G - \frac{\left(m_k^{\Sigma} v_{Ck}^{\Delta} + m_k^{\Delta} v_{Ck}^{\Sigma}\right)}{4} - R_\delta i_k^{\Delta} \tag{1d}$$

Moreover, the control variables are represented by $m_k^{\Sigma} = m_k^U + m_k^L$ and $m_k^{\Delta} = m_k^U - m_k^L$, where m_k^U and m_k^L are respectively the upper and lower arms insertion indexes. Finally, an equivalent ac inductance and resistance are conveniently defined as $L_\delta = L_\sigma/2 + L_f$ and $R_\delta = R_\sigma/2 + R_f$.

2) State variable frequency classification: A frequency analysis can be performed by briefly assuming that m_k^U is phase-shifted approximately $180°$ with respect to m_k^L, resulting in $m_k^{\Sigma} \approx 1$ and $m_k^{\Delta} \approx \hat{m} cos\,(\omega t)$. By inspecting the right-side of (1a), and further assuming a grid current i_k^{Δ} oscillating at ω, it can be seen that in steady-state, the first product $m_k^{\Delta} i_k^{\Delta}/2$ consists on a product of two sinusoidal signals oscillating at ω resulting in a 2ω sinusoidal signal plus an offset. In addition, the second product $m_k^{\Sigma} i_k^{\Sigma}$ gives a DC value in the case CCSC presented in [21] is used or a 2ω signal otherwise, resulting for both cases in 2ω oscillations for v_{Ck}^{Σ}, in addition to a dc component. Similarly for v_{Ck}^{Δ}, the first product on the right-side of (1b) $m_k^{\Sigma} i_k^{\Delta}/2$ oscillates at ω, while the second product $m_k^{\Delta} i_k^{\Sigma}$ oscillates at ω in the case the CCSC is used or will result in a signal oscillating at ω superimposed to one at 3ω otherwise. Finally, notice that a similar analysis can be made for the current dynamics. This leads to an initial frequency classification of the state and control variables of the converter based on their steady-state dynamic oscillations, as summarized in table I. Furthermore, notice that this table does not include the dc components or the third harmonic oscillation information, as both of these frequencies are later conveniently extracted by means of the zero-sequence of each variable.

TABLE I. MMC VARIABLES IN Σ-Δ REPRESENTATION

Variables oscillating at ω	Variables oscillating at -2ω
$i_k^{\Delta} = i_k^U - i_k^L$	$i_k^{\Sigma} = (i_k^U + i_k^L)/2$
$v_{Ck}^{\Delta} = (-v_{Ck}^U + v_{Ck}^L)$	$v_{Ck}^{\Sigma} = (v_{Ck}^U + v_{Ck}^L)$
$m_k^{\Delta} = m_k^U - m_k^L$	$m_k^{\Sigma} = m_k^U + m_k^L$

3) Application of Park's transformations at different frequencies: Based on this initial classification; i.e., Σ-state and control variables oscillate mainly at 2ω whereas Δ variables oscillate at ω, the strategy depicted in Fig. 2 is implemented. More precisely, Park's transformation $\boldsymbol{P_{-2\omega}}$ at 2ω is applied to all the Σ vector variables $\boldsymbol{v_{Cabc}^{\Sigma}}$, $\boldsymbol{i_{abc}^{\Sigma}}$ and $\boldsymbol{m_{abc}^{\Sigma}}$. Conversely, Park's transformation $\boldsymbol{P_{\omega}}$ at ω is applied to the Δ vector variables $\boldsymbol{v_{Cabc}^{\Delta}}$, $\boldsymbol{i_{abc}^{\Delta}}$ and $\boldsymbol{m_{abc}^{\Delta}}$. Furthermore, since the zero-sequence v_{Cz}^{Δ} is still SSTP at 3ω, a virtual signal is created shifted $90°$ with respect to the original one as indicated in Fig. 2, such that an additional Park transformation $\boldsymbol{P_{3\omega}}$ at 3ω can be used to transform the SSTP vector $\left[v_{Cz}^{\Delta}, v_{Cz}^{\Delta 90°}\right]^{\top}$ into the SSTI one $\left[v_{CZ_d}^{\Delta}, v_{CZ_q}^{\Delta}\right]^{\top}$.

By further replacing all the definitions given in Fig. 2 in the three phase equivalent dynamic equations given in (1), the structure-preserving SSTI model proposed in [8] is obtained. The resulting model is also recalled in the next section, although directly from a Port-Hamiltonian viewpoint.

III. PORT-HAMILTONIAN MODELLING LIMITATIONS OF THE SSTI MODEL OF THE MMC

A. Port-Hamiltonian modelling

The state-space equations of certain dynamical systems can be represented by means of the port-Hamiltonian formalism, as follows:

$$\dot{\boldsymbol{x}} = \left(\boldsymbol{J}_0 + \sum_{i=1}^{m} \boldsymbol{J}_i u_i - \boldsymbol{R}\right) \boldsymbol{\nabla} H\left(\boldsymbol{x}\right) + \boldsymbol{E} \tag{2}$$

where $\boldsymbol{x} \in \Re^n$ is the state vector, and $\boldsymbol{u} \in \Re^m$ denotes the control vector. Furthermore, $\boldsymbol{R} = \boldsymbol{R}^{\top} \geq 0$ is the

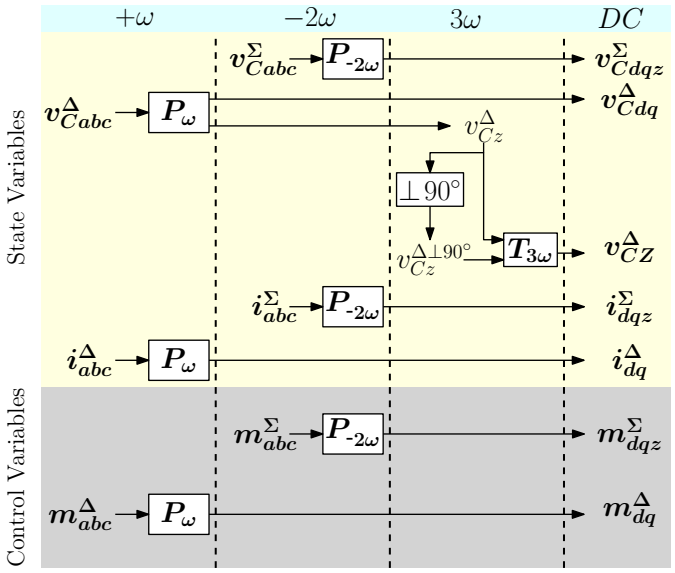

Fig. 2. The proposed modelling approach based on three Park transformations to achieve SSTI control and state variables

dissipation matrix whereas $\boldsymbol{J}_0 = \boldsymbol{J}_0^\top$ and $\boldsymbol{J}_i = -\boldsymbol{J}_i^\top$ are the power preserving skew-symmetric interconnection matrices of the system. Moreover, the operator $\boldsymbol{\nabla} = \dfrac{\partial}{\partial \boldsymbol{x}}$, is acting on the energy $H(\boldsymbol{x})$ stored in the system, which is defined as

$$H\left(\boldsymbol{x}\right) = \frac{1}{2}\boldsymbol{x}^\top \boldsymbol{Q}\boldsymbol{x}, \tag{3}$$

where $\boldsymbol{Q} = \boldsymbol{Q}^\top > 0$ is a symmetrical matrix with the energy storing element parameters. Finally, the vector $\boldsymbol{E}$ contains the external sources of the system.

B. Limitations of the SSTI MMC model for port-Hamiltonian representation

A first attempt to represent the state-space equations of the SSTI MMC model proposed in [8] under the mathematical formalism given in (2) is here presented.

The first step is to define the state vector $\boldsymbol{x}$ of this model. Following the methodology presented in [3], it is convenient to define the state vector in terms of charges q and fluxes ϕ, instead of the commonly utilized voltages v and currents i. The relationship between both representations is straightforward since $q = Cv$ and $\phi = Li$ where C and L are respectively a general capacitance and inductance. Therefore, the state vector $\boldsymbol{x}$ of the MMC is represented as in (4), where the SSTI vectors $\boldsymbol{q}^{\boldsymbol{\Sigma}}_{\boldsymbol{Cdqz}}$, $\boldsymbol{q}^{\boldsymbol{\Delta}}_{\boldsymbol{CdqZ}}$, $\boldsymbol{\phi}^{\boldsymbol{\Sigma}}_{\boldsymbol{dqz}}$ and $\boldsymbol{\phi}^{\boldsymbol{\Delta}}_{\boldsymbol{dq}}$ defined in (5a) can be easily expressed as a function of the respective SSTI vectors $\boldsymbol{v}^{\boldsymbol{\Sigma}}_{\boldsymbol{Cdqz}}$, $\boldsymbol{v}^{\boldsymbol{\Delta}}_{\boldsymbol{CdqZ}}$, $\boldsymbol{i}^{\boldsymbol{\Sigma}}_{\boldsymbol{dqz}}$ and $\boldsymbol{i}^{\boldsymbol{\Delta}}_{\boldsymbol{dq}}$ used in [8] and recalled in (5b), as indicated by the second equality in (4).

$$\boldsymbol{x} = \begin{bmatrix} \boldsymbol{q}^{\boldsymbol{\Sigma}}_{\boldsymbol{Cdqz}} \\ \boldsymbol{q}^{\boldsymbol{\Delta}}_{\boldsymbol{CdqZ}} \\ \boldsymbol{\phi}^{\boldsymbol{\Sigma}}_{\boldsymbol{dqz}} \\ \boldsymbol{\phi}^{\boldsymbol{\Delta}}_{\boldsymbol{dq}} \end{bmatrix} = \begin{bmatrix} C_\sigma \boldsymbol{v}^{\boldsymbol{\Sigma}}_{\boldsymbol{Cdqz}} \\ C_\sigma \boldsymbol{q}^{\boldsymbol{\Delta}}_{\boldsymbol{CdqZ}} \\ L_\sigma \boldsymbol{i}^{\boldsymbol{\Sigma}}_{\boldsymbol{dqz}} \\ L_\delta \boldsymbol{i}^{\boldsymbol{\Delta}}_{\boldsymbol{dq}} \end{bmatrix} \tag{4}$$

$$\boldsymbol{q}^{\boldsymbol{\Sigma}}_{\boldsymbol{Cdqz}} = \begin{bmatrix} q^{\Sigma}_{Cd} & q^{\Sigma}_{Cq} & q^{\Sigma}_{Cz} \end{bmatrix}^\top, \quad \boldsymbol{\phi}^{\boldsymbol{\Sigma}}_{\boldsymbol{dqz}} = \begin{bmatrix} \phi^{\Sigma}_{d} & \phi^{\Sigma}_{q} & \phi^{\Sigma}_{z} \end{bmatrix}^\top,$$
$$\boldsymbol{q}^{\boldsymbol{\Delta}}_{\boldsymbol{CdqZ}} = \begin{bmatrix} q^{\Delta}_{Cd} & q^{\Delta}_{Cq} & q^{\Delta}_{CZ_d} & q^{\Delta}_{CZ_q} \end{bmatrix}^\top, \quad \boldsymbol{\phi}^{\boldsymbol{\Delta}}_{\boldsymbol{dq}} = \begin{bmatrix} \phi^{\Delta}_{d} & \phi^{\Delta}_{q} \end{bmatrix}^\top, \tag{5a}$$

$$\boldsymbol{v}^{\boldsymbol{\Sigma}}_{\boldsymbol{Cdqz}} = \begin{bmatrix} v^{\Sigma}_{Cd} & v^{\Sigma}_{Cq} & v^{\Sigma}_{Cz} \end{bmatrix}^\top, \quad \boldsymbol{i}^{\boldsymbol{\Sigma}}_{\boldsymbol{dqz}} = \begin{bmatrix} i^{\Sigma}_{d} & i^{\Sigma}_{q} & i^{\Sigma}_{z} \end{bmatrix}^\top,$$
$$\boldsymbol{v}^{\boldsymbol{\Delta}}_{\boldsymbol{CdqZ}} = \begin{bmatrix} v^{\Delta}_{Cd} & v^{\Delta}_{Cq} & v^{\Delta}_{CZ_d} & v^{\Delta}_{CZ_q} \end{bmatrix}^\top, \quad \boldsymbol{i}^{\boldsymbol{\Delta}}_{\boldsymbol{dq}} = \begin{bmatrix} i^{\Delta}_{d} & i^{\Delta}_{q} \end{bmatrix}^\top, \tag{5b}$$

The control vector $\boldsymbol{u} = [u_1, \ldots, u_m]^\top$ in (2) is in turn represented by the five SSTI modulation indexes of the SSTI MMC model of [8] as suggested in (6a), where $\boldsymbol{m}^{\boldsymbol{\Sigma}}_{\boldsymbol{dqz}}$ and $\boldsymbol{m}^{\boldsymbol{\Delta}}_{\boldsymbol{dq}}$ are defined as in (6b).

$$\boldsymbol{u} = \begin{bmatrix} \boldsymbol{m}^{\boldsymbol{\Sigma}}_{\boldsymbol{dqz}} \\ \boldsymbol{m}^{\boldsymbol{\Delta}}_{\boldsymbol{dq}} \end{bmatrix} \tag{6a}$$

$$\boldsymbol{m}^{\boldsymbol{\Sigma}}_{\boldsymbol{dqz}} = \begin{bmatrix} m^{\Sigma}_{d} & m^{\Sigma}_{q} & m^{\Sigma}_{z} \end{bmatrix}^\top, \quad \boldsymbol{m}^{\boldsymbol{\Delta}}_{\boldsymbol{dq}} = \begin{bmatrix} m^{\Delta}_{d} & m^{\Delta}_{q} \end{bmatrix}^\top \tag{6b}$$

Furthermore, the total stored energy in the system under consideration; or what is the same, the Hamiltonian function $H(\boldsymbol{x})$, needs to be identified for the SSTI MMC model using the formalism given in (3). For the system under consideration, the energy storing devices are the MMC inductances and capacitances. More precisely, seven capacitances with a value of C_σ; i.e., one associated to each of the sum and difference voltages defined in (5b), three inductances with value L_σ associated to the circulating current vector, as well as two additional inductances with value L_δ associated to the grid current vector, both defined in (5b) as well. Taking into account that the Hamiltonian function for a generic system with one capacitance C and one inductance L can be defined as $\frac{1}{2}(Cv^2 + Li^2)$, and that it can be further expressed as $\frac{1}{2}(C^{-1}q^2 + L^{-1}\phi^2)$ using the charges-voltages and flux-current relationships, the Hamiltonian function for the system under study can therefore be expressed as in (3), where $\boldsymbol{x}$ are the charges and fluxes of the SSTI MMC previously defined in (4), and $\boldsymbol{Q}$ is the 12×12 diagonal matrix given in (7).

$$\boldsymbol{Q} = \operatorname{diag}(\underbrace{C_\sigma^{-1}, \ldots, C_\sigma^{-1}}_{1\times 7}, \underbrace{L_\sigma^{-1}, \ldots, L_\sigma^{-1}}_{1\times 3}, \underbrace{L_\delta^{-1}, L_\delta^{-1}}_{1\times 2}) \tag{7}$$

As can be seen from (2), it is necessary to further determine the gradient of the Hamiltonian function; i.e., $\boldsymbol{\nabla} H(\boldsymbol{x})$, where $\boldsymbol{\nabla}$ is the operator represented by $\partial/\partial \boldsymbol{x}$. Hence, by differentiating the Hamiltonian function with respect to all the states, the vector $\boldsymbol{\nabla} H(\boldsymbol{x})$ can be expressed as in (8). Notice that this gives a vector containing all the voltages and currents of the system, as suggested by the second equality of this equation.

$$\begin{aligned}\boldsymbol{\nabla} H\left(\boldsymbol{x}\right) &= \begin{bmatrix} \dfrac{\boldsymbol{q}_{\boldsymbol{Cdqz}}^{\boldsymbol{\Sigma}\top}}{C_\sigma} & \dfrac{\boldsymbol{q}_{\boldsymbol{CdqZ}}^{\boldsymbol{\Delta}\top}}{C_\sigma} & \dfrac{\boldsymbol{\phi}_{\boldsymbol{dqz}}^{\boldsymbol{\Sigma}\top}}{L_\sigma} & \dfrac{\boldsymbol{\phi}_{\boldsymbol{dq}}^{\boldsymbol{\Delta}\top}}{L_\delta} \end{bmatrix}^\top \\ &= \begin{bmatrix} \boldsymbol{v}_{\boldsymbol{Cdqz}}^{\boldsymbol{\Sigma}\top} & \boldsymbol{v}_{\boldsymbol{CdqZ}}^{\boldsymbol{\Delta}\top} & \boldsymbol{i}_{\boldsymbol{dqz}}^{\boldsymbol{\Sigma}\top} & \boldsymbol{i}_{\boldsymbol{dq}}^{\boldsymbol{\Delta}\top} \end{bmatrix}^\top \end{aligned} \tag{8}$$

Having identified the gradient of the Hamiltonian as the vector of voltages and currents of the system under consideration, the vector $\boldsymbol{E}$ can be easily identified from the SSTI MMC model of [8] as it represents all of the elements that are not being multiplied by $\boldsymbol{\nabla} H(\boldsymbol{x})$. This leaves only the ac and dc sources ($\boldsymbol{v}_{\boldsymbol{dq}}^{\boldsymbol{G}}$ and v_{dc}) of the converter, as expressed in (9).

$$\boldsymbol{E} = \left[\begin{array}{c:ccc} \mathbf{0}_{1\times 9} & \frac{1}{2}v_{dc} & -v_d^G & -v_q^G \end{array}\right]^\top \tag{9}$$

Conversely, the rest of the system, represented by the matrix $(\boldsymbol{J}_0 + \sum_{i=1}^{m} \boldsymbol{J}_i u_i - \boldsymbol{R})$, can be easily identified from [8], as it the part of the dynamics that is being multiplied by $\boldsymbol{\nabla} H(\boldsymbol{x})$. Before assessing each of the individual elements ($\boldsymbol{R}$, $\boldsymbol{J}_0$ and $\boldsymbol{J}_i$) the full matrix is given in (10) for convenience.

It is possible to easily extract from (10) the dissipation matrix $\boldsymbol{R}$ as in (11), from where it can be seen that the dissipation elements are only associated to the currents of the system, and that as expected $\boldsymbol{R} = \boldsymbol{R}^\top$.

$$\boldsymbol{R} = \left[\begin{array}{c:ccccc} \mathbf{0}_{7\times 7} & \multicolumn{5}{c}{\mathbf{0}_{7\times 5}} \\ \hdashline & R_\sigma & 0 & 0 & 0 & 0 \\ & 0 & R_\sigma & 0 & 0 & 0 \\ \mathbf{0}_{5\times 7} & 0 & 0 & R_\sigma & 0 & 0 \\ & 0 & 0 & 0 & R_\delta & 0 \\ & 0 & 0 & 0 & 0 & R_\delta \end{array}\right] \tag{11}$$

Moreover, the interconnection matrix $\boldsymbol{J}_0$ of the port-Hamiltonian modelling formalism can be extracted from (10), by identifying the non-resistive elements that are being multiplied by the voltage and current variables, without any participation from the control vector $\boldsymbol{u}$, as suggested in (2). From this procedure, $\boldsymbol{J}_0$ is identified as the block diagonal 12×12 matrix associated to all the cross-coupling terms of the SSTI MMC model dynamics, as given in (12a), where $\boldsymbol{J}_0^C$ is the upper block diagonal sub-matrix given in (12b) corresponding to the capacitor elements, whereas $\boldsymbol{J}_0^L$ is the lower sub-matrix given in (12c) which corresponds to the inductive elements.

$$\boldsymbol{J}_0 = \left[\begin{array}{c:c} \boldsymbol{J}_0^C & \mathbf{0}_{7\times 5} \\ \hdashline \mathbf{0}_{5\times 7} & \boldsymbol{J}_0^L \end{array}\right]_{12\times 12} \tag{12a}$$

$$\boldsymbol{J}_0^C = \omega \begin{bmatrix} 0 & 2C_\sigma & 0 & 0 & 0 & 0 & 0 \\ -2C_\sigma & 0 & 0 & 0 & 0 & 0 & 0 \\ 0 & 0 & 0 & 0 & 0 & 0 & 0 \\ 0 & 0 & 0 & 0 & C_\sigma & 0 & 0 \\ 0 & 0 & 0 & -C_\sigma & 0 & 0 & 0 \\ 0 & 0 & 0 & 0 & 0 & 0 & 3C_\sigma \\ 0 & 0 & 0 & 0 & 0 & -3C_\sigma & 0 \end{bmatrix} \tag{12b}$$

$$\boldsymbol{J}_0^L = \omega \begin{bmatrix} 0 & 2L_\sigma & 0 & 0 & 0 \\ -2L_\sigma & 0 & 0 & 0 & 0 \\ 0 & 0 & 0 & 0 & 0 \\ 0 & 0 & 0 & 0 & L_\delta \\ 0 & 0 & 0 & -L_\delta & 0 \end{bmatrix} \tag{12c}$$

Notice that $\boldsymbol{J}_0$ is skew-symmetric as required by the port-Hamiltonian modelling formalism, since $\boldsymbol{J}_0 = -\boldsymbol{J}_0^\top$; or equivalently, $\boldsymbol{J}_0^C = -\boldsymbol{J}_0^{C\top}$ and $\boldsymbol{J}_0^L = -\boldsymbol{J}_0^{L\top}$.

Similarly, all the interconnection matrices $\boldsymbol{J}_i$ can be extracted from (10). Notice that there are five of these matrices, as there is one matrix for each of the $m = 5$ control variables defined in (16) and (6b). Furthermore, by simple inspection of (10), it is possible to see that all of the five $\boldsymbol{J}_i$ matrices have the structure represented by (13a), as no control variables appear in the block diagonal part of (10).

$$\boldsymbol{J}_i = \left[\begin{array}{c:c} \mathbf{0}_{7\times 7} & \boldsymbol{J}_i^C \\ \hdashline \boldsymbol{J}_i^L & \mathbf{0}_{5\times 5} \end{array}\right], \; for\; i = 1 \ldots m. \tag{13a}$$

Notice that skew-symmetry is achieved if $\boldsymbol{J}_i = -\boldsymbol{J}_i^\top$. Furthermore, since the negative transpose matrix $-\boldsymbol{J}_i^\top$ can be defined as in (13b), it can be concluded by equalizing (13a) with (13b) that $\boldsymbol{J}_i$ is skew-symmetric; i.e., $\boldsymbol{J}_i = -\boldsymbol{J}_i^\top$ if the internal sub-matrices of $\boldsymbol{J}_i$ comply with $\boldsymbol{J}_i^C = -\boldsymbol{J}_i^{L\top}$.

$$-\boldsymbol{J}_i^\top = \left[\begin{array}{c:c} \mathbf{0}_{7\times 7} & -\boldsymbol{J}_i^L \\ \hdashline -\boldsymbol{J}_i^C & \mathbf{0}_{5\times 5} \end{array}\right], \; for\; i = 1 \ldots m. \tag{13b}$$

For the case $i = 1$, the interconnection matrix associated to first control variable $u_1 = m_d^\Sigma$ is extracted from (10), resulting in the two sub-matrices given in (14a).

$$\overbrace{\begin{bmatrix} 0 & 0 & 1 & 0 & 0 \\ 0 & 0 & 0 & 0 & 0 \\ \frac{1}{2} & 0 & 0 & 0 & 0 \\ 0 & 0 & 0 & \frac{1}{4} & 0 \\ 0 & 0 & 0 & 0 & -\frac{1}{4} \\ 0 & 0 & 0 & \frac{1}{4} & 0 \\ 0 & 0 & 0 & 0 & \frac{1}{4} \end{bmatrix}}^{\boldsymbol{J}_1^C}; \quad \overbrace{\begin{bmatrix} 0 & 0 & -\frac{1}{4} & 0 & 0 & 0 & 0 \\ 0 & 0 & 0 & 0 & 0 & 0 & 0 \\ -\frac{1}{8} & 0 & 0 & 0 & 0 & 0 & 0 \\ 0 & 0 & 0 & -\frac{1}{8} & 0 & -\frac{1}{8} & 0 \\ 0 & 0 & 0 & 0 & \frac{1}{8} & 0 & -\frac{1}{8} \end{bmatrix}}^{\boldsymbol{J}_1^L} \tag{14a}$$

$$\left(\boldsymbol{J}_0 + \sum_{i=1}^{m} \boldsymbol{J}_i \boldsymbol{u}_i - \boldsymbol{R}\right) = \ldots \tag{10}$$

$$\left[\begin{array}{ccccccc:ccccc}
0 & C_\sigma 2\omega & 0 & 0 & 0 & 0 & 0 & m_z^\Sigma & 0 & m_d^\Sigma & \frac{m_d^\Delta}{4} & -\frac{m_q^\Delta}{4} \\
-C_\sigma 2\omega & 0 & 0 & 0 & 0 & 0 & 0 & 0 & m_z^\Sigma & m_q^\Sigma & \frac{m_q^\Delta}{4} & \frac{m_d^\Delta}{4} \\
0 & 0 & 0 & 0 & 0 & 0 & 0 & \frac{m_d^\Sigma}{2} & \frac{m_q^\Sigma}{2} & m_z^\Sigma & \frac{m_d^\Delta}{4} & \frac{m_q^\Delta}{4} \\
0 & 0 & 0 & 0 & C_\sigma\omega & 0 & 0 & \frac{m_d^\Delta}{2} & \frac{m_q^\Delta}{2} & m_d^\Delta & \frac{m_d^\Sigma}{4}+\frac{m_z^\Sigma}{2} & \frac{m_q^\Sigma}{4} \\
0 & 0 & 0 & -C_\sigma\omega & 0 & 0 & 0 & -\frac{m_q^\Delta}{2} & \frac{m_d^\Delta}{2} & m_q^\Delta & \frac{m_q^\Sigma}{4} & \frac{m_z^\Sigma}{2}-\frac{m_d^\Sigma}{4} \\
0 & 0 & 0 & 0 & 0 & 0 & C_\sigma 3\omega & \frac{m_d^\Delta}{2} & -\frac{m_q^\Delta}{2} & 0 & \frac{m_d^\Sigma}{4} & -\frac{m_q^\Sigma}{4} \\
0 & 0 & 0 & 0 & 0 & -C_\sigma 3\omega & 0 & \frac{m_q^\Delta}{2} & \frac{m_d^\Delta}{2} & 0 & \frac{m_q^\Sigma}{4} & \frac{m_d^\Sigma}{4} \\
\hdashline
-\frac{m_z^\Sigma}{4} & 0 & -\frac{m_d^\Sigma}{4} & -\frac{m_d^\Delta}{8} & \frac{m_q^\Delta}{8} & -\frac{m_d^\Delta}{8} & -\frac{m_q^\Delta}{8} & -R_\sigma & L_\sigma 2\omega & 0 & 0 & 0 \\
0 & -\frac{m_z^\Sigma}{4} & -\frac{m_q^\Sigma}{4} & -\frac{m_q^\Delta}{8} & -\frac{m_d^\Delta}{8} & \frac{m_q^\Delta}{8} & -\frac{m_d^\Delta}{8} & -L_\sigma 2\omega & -R_\sigma & 0 & 0 & 0 \\
-\frac{m_d^\Sigma}{8} & -\frac{m_q^\Sigma}{8} & -\frac{m_z^\Sigma}{4} & -\frac{m_d^\Delta}{8} & -\frac{m_q^\Delta}{8} & 0 & 0 & 0 & 0 & -R_\sigma & 0 & 0 \\
-\frac{m_d^\Delta}{8} & -\frac{m_q^\Delta}{8} & -\frac{m_d^\Delta}{4} & -\frac{m_d^\Sigma}{8}-\frac{m_z^\Sigma}{4} & -\frac{m_q^\Sigma}{8} & -\frac{m_d^\Sigma}{8} & -\frac{m_q^\Sigma}{8} & 0 & 0 & 0 & -R_\delta & L_\delta\omega \\
\frac{m_q^\Delta}{8} & -\frac{m_d^\Delta}{8} & -\frac{m_q^\Delta}{4} & -\frac{m_q^\Sigma}{8} & \frac{m_d^\Sigma}{8}-\frac{m_z^\Sigma}{4} & \frac{m_q^\Sigma}{8} & -\frac{m_d^\Sigma}{8} & 0 & 0 & 0 & -L_\delta\omega & -R_\delta
\end{array}\right]$$

It can be seen that $\boldsymbol{J}_1^C \neq -\boldsymbol{J}_1^{L\top}$, or similarly that $\boldsymbol{J}_1 \neq -\boldsymbol{J}_1^\top$. In addition, it is possible to observe as well that they are not skew-symmetric due to the different values of the gains in both sub-matrices, despite having the desired signs. Moreover, identical observations can be made for the rest of the control related interconnection (sub-)matrices $\boldsymbol{J}_2$, $\boldsymbol{J}_3$, $\boldsymbol{J}_4$, and $\boldsymbol{J}_5$, which are respectively associated to $u_2 = m_q^\Sigma$, $u_3 = m_z^\Sigma$, $u_4 = m_d^\Delta$ and $u_5 = m_q^\Delta$, given in (14b), (14c), (14d) and (14e), respectively. Therefore, it can be concluded that none of the five control-related interconnection matrices $\boldsymbol{J}_i$ are skew-symmetric. Since skew-symmetry of these matrices is a requirement for a port-Hamiltonian representation, the SSTI MMC model of [8] is not directly suited for such formalism without additional mathematical manipulation.

$$\overbrace{\begin{bmatrix} 0&0&0&0&0 \\ 0&0&1&0&0 \\ 0&\frac{1}{2}&0&0&0 \\ 0&0&0&0&\frac{1}{4} \\ 0&0&0&\frac{1}{4}&0 \\ 0&0&0&0&-\frac{1}{4} \\ 0&0&0&\frac{1}{4}&0 \end{bmatrix}}^{\boldsymbol{J}_2^C}
\overbrace{\begin{bmatrix} 0&0&0&0&0&0&0 \\ 0&0&-\frac{1}{4}&0&0&0&0 \\ 0&-\frac{1}{8}&0&0&0&0&0 \\ 0&0&0&0&-\frac{1}{8}&0&-\frac{1}{8} \\ 0&0&0&-\frac{1}{8}&0&\frac{1}{8}&0 \end{bmatrix}}^{\boldsymbol{J}_2^L} \tag{14b}$$

$$\overbrace{\begin{bmatrix} 1&0&0&0&0 \\ 0&1&0&0&0 \\ 0&0&1&0&0 \\ 0&0&0&\frac{1}{2}&0 \\ 0&0&0&0&\frac{1}{2} \\ 0&0&0&0&0 \\ 0&0&0&0&0 \end{bmatrix}}^{\boldsymbol{J}_3^C}
\overbrace{\begin{bmatrix} -\frac{1}{4}&0&0&0&0&0&0 \\ 0&-\frac{1}{4}&0&0&0&0&0 \\ 0&0&-\frac{1}{4}&0&0&0&0 \\ 0&0&0&-\frac{1}{4}&0&0&0 \\ 0&0&0&0&-\frac{1}{4}&0&0 \end{bmatrix}}^{\boldsymbol{J}_3^L} \tag{14c}$$

$$\overbrace{\begin{bmatrix} 0 & 0 & 0 & \frac{1}{4} & 0 \\ 0 & 0 & 0 & 0 & \frac{1}{4} \\ 0 & 0 & 0 & \frac{1}{4} & 0 \\ \frac{1}{2} & 0 & 1 & 0 & 0 \\ 0 & \frac{1}{2} & 0 & 0 & 0 \\ \frac{1}{2} & 0 & 0 & 0 & 0 \\ 0 & \frac{1}{2} & 0 & 0 & 0 \end{bmatrix}}^{\boldsymbol{J}_4^C} \overbrace{\begin{bmatrix} 0 & 0 & 0 & -\frac{1}{8} & 0 & -\frac{1}{8} & 0 \\ 0 & 0 & 0 & 0 & -\frac{1}{8} & 0 & -\frac{1}{8} \\ 0 & 0 & 0 & -\frac{1}{8} & 0 & 0 & 0 \\ -\frac{1}{8} & 0 & -\frac{1}{4} & 0 & 0 & 0 & 0 \\ 0 & -\frac{1}{8} & 0 & 0 & 0 & 0 & 0 \end{bmatrix}}^{\boldsymbol{J}_4^L} \tag{14d}$$

$$\overbrace{\begin{bmatrix} 0 & 0 & 0 & 0 & -\frac{1}{4} \\ 0 & 0 & 0 & \frac{1}{4} & 0 \\ 0 & 0 & 0 & 0 & \frac{1}{4} \\ 0 & \frac{1}{2} & 0 & 0 & 0 \\ -\frac{1}{2} & 0 & 1 & 0 & 0 \\ 0 & -\frac{1}{2} & 0 & 0 & 0 \\ \frac{1}{2} & 0 & 0 & 0 & 0 \end{bmatrix}}^{\boldsymbol{J}_5^C} \overbrace{\begin{bmatrix} 0 & 0 & 0 & 0 & \frac{1}{8} & 0 & -\frac{1}{8} \\ 0 & 0 & 0 & -\frac{1}{8} & 0 & \frac{1}{8} & 0 \\ 0 & 0 & 0 & 0 & -\frac{1}{8} & 0 & 0 \\ 0 & -\frac{1}{8} & 0 & 0 & 0 & 0 & 0 \\ \frac{1}{8} & 0 & -\frac{1}{4} & 0 & 0 & 0 & 0 \end{bmatrix}}^{\boldsymbol{J}_5^L} \tag{14e}$$

IV. Proposed mathematical manipulations for port-Hamiltonian MMC modelling with skew-symmetric matrices

A. Pattern identifications and proposed modifications

In order to overcome the obstacle introduced by the lack of skew-symmetry of the control-related interconnection matrices $\boldsymbol{J}_0$ for expressing the SSTI MMC model in a port-Hamiltonian framework, the following methodology is proposed.

1) Change of variables associated to the zero-sequence: The proposed change consists on defining new zero-sequence related control and state variables $\hat{m}_z^\Sigma = 2m_z^\Sigma$, $\hat{i}_z^\Sigma = 2i_z^\Sigma$ and $\hat{v}_{Cz}^\Sigma = 2v_{Cz}^\Sigma$.

This change of variables will modify the structure of (10) by adding an additional gain of $\frac{1}{2}$ to any component that was previously being multiplied by any of the original zero-sequence variables. This change will result in a matrix where the $\frac{1}{4}$ gains associated to the grid currents $\boldsymbol{i}_{\boldsymbol{dq}}^{\boldsymbol{\Delta}}$ corresponding to the eleventh and twelfth column of the upper-right sub-matrix of (10), will be half of the gain associated to the circulating current $\frac{1}{2}$, found in the eighth, ninth and tenth column of the upper-right sub-matrix of (10). Notice that the only exception of the above described effect occurs when two zero sequence variables multiply each other, as is the case for the element on the third row and tenth column of (10), as the new insertion index $\hat{m}_z^\Sigma$ will be multiplying the new definition of the zero-sequence circulating current $\hat{i}_z^\Sigma$.

Moreover, this same change of variables will make the gain $\frac{1}{8}$ common to all the elements of the lower-left sub-matrix of (10). Notice that the here too, one exception can be found which is also caused when two zero sequence variables multiply each other, as is the case of the element in the tenth row and third column of (10), where the new insertion index $\hat{m}_z^\Sigma$ is multiplying the new definition of the zero-sequence voltage sum $\hat{v}_{Cz}^\Sigma$.

2) Change of variables associated to the system parameters: This second change of variable aims at simplifying the resulting gains, and consists of conveniently redefining the system capacitances, inductances and resistances. More precisely, it is proposed to use $\hat{C}_\sigma = 2C_\sigma$, $\hat{C}_{\sigma z} = C_\sigma$, $\hat{L}_\sigma = 8L_\sigma$, $\hat{R}_\sigma = 8R_\sigma$, $\hat{L}_{\sigma z} = 4L_\sigma$, $\hat{R}_{\sigma z} = 4R_\sigma$, $\hat{L}_\delta = 8L_\delta$ and $\hat{L}_\delta = R_\delta$. Notice that the parameters $\hat{C}_{\sigma z}$, $\hat{L}_{\sigma z}$ and $\hat{R}_{\sigma z}$, which are those associated to the zero-sequence dynamics, are different from their counterparts.

3) Per unit system definition: Finally, a per unit system is adopted with the aim of normalizing all of the gains. This is particularly useful to address the issue of the grid currents having half the gain values of the circulating current, as consequence of the first variable change proposed. This is done by properly selecting the the base of the apparent power as $S_B = 3V_B \cdot I_{\Delta B} = V_{Bdc} \cdot I_{Bdc}$, where V_B and $I_{\Delta B}$ are the ac-side base voltage and current base values and V_{Bdc} and I_{Bdc} are their dc-side counterparts. By further defining V_{Bdc} as $2V_B$ and the circulating current base $I_{\Sigma B}$ as $\frac{1}{3}I_{Bdc}$, it is possible to obtain the expression of $I_{\Sigma B}$ as a function of $I_{\Delta B}$ as: $I_{\Sigma B} = \frac{1}{2}I_{\Delta B}$. By using this last relationship, it is possible to normalize most of the terms in the upper-right side of (10), by using $\boldsymbol{i}_{\boldsymbol{dqz}}^{\boldsymbol{\Sigma}pu} = \boldsymbol{i}_{\boldsymbol{dqz}}^{\boldsymbol{\Sigma}}/I_{\Sigma B}$, and $\boldsymbol{i}_{\boldsymbol{dq}}^{\boldsymbol{\Delta}pu} = \boldsymbol{i}_{\boldsymbol{dq}}^{\boldsymbol{\Delta}}/I_{\Delta B}$. Similarly, a voltage sum base $V_{\Sigma B}$ defined as $4V_B$ can be used to normalize the voltages as $\boldsymbol{v}_{\boldsymbol{Cdq}}^{\boldsymbol{\Sigma}pu} = \boldsymbol{v}_{\boldsymbol{Cdq}}^{\boldsymbol{\Sigma}}/V_{\Sigma B}$, $\hat{v}_{Cz}^{\Sigma pu} = \hat{v}_{Cz}^\Sigma/V_{\Sigma B}$ and $\boldsymbol{v}_{\boldsymbol{Cdq}}^{\boldsymbol{\Delta}pu} = \boldsymbol{v}_{\boldsymbol{Cdq}}^{\boldsymbol{\Delta}}/V_{\Sigma B}$.

In addition, since $V_{\Sigma B} = 4V_B = 4Z_B I_{\Delta B} = 8Z_B I_{\Sigma B} = Z_{\Sigma B} I_{\Sigma B} = \omega_b 8L_B I_{\Sigma B} = \omega_b L_{\Sigma B} I_{\Sigma B}$, it is also possible to define $\hat{R}_\sigma^{pu} = \hat{R}_\sigma/Z_{\Sigma B}$, $\hat{L}_\sigma^{pu} = \hat{L}_\sigma/L_{\Sigma B}$, $\hat{R}_{\sigma z}/Z_{\Sigma B}$ and $\hat{L}_{\sigma z}^{pu} = \hat{L}_\sigma/L_{\Sigma B}$. Finally, given that $I_{\Sigma B} = I_{\Delta B}/2 = V_B\omega_b C_B/2 = V_{\Sigma B}\omega_b C_b/8 = V_{\Sigma B}\omega_b C_{\Sigma B}$, the capacitors can be defined using per unit notation as $\hat{C}_\sigma^{pu} = \hat{C}_\sigma/C_{\Sigma B}$ and $\hat{C}_{\sigma z}^{pu} = \hat{C}_{\sigma z}/C_{\Sigma B}$.

B. Port-Hamiltonian modelling with the proposed changes

Applying the proposed changes leads to a new port-Hamiltonian representation which is presented in this section. However, due to the implementation of the proposed variable changes, it is necessary to redefine the elements in (2). First, the new state variable vector $\boldsymbol{x}$ is given in (15), where the new per unit expressions of the charges and fluxes are defined based on the new per unit

expressions of the voltages, currents and their associated parameters.

$$\boldsymbol{x} = \begin{bmatrix} \boldsymbol{q}_{\boldsymbol{Cdq}}^{\boldsymbol{\Sigma}pu} \\ \hat{q}_{Cz}^{\Sigma pu} \\ \hline \boldsymbol{q}_{\boldsymbol{CdqZ}}^{\boldsymbol{\Delta}pu} \\ \hline \boldsymbol{\phi}_{\boldsymbol{dq}}^{\boldsymbol{\Sigma}pu} \\ \hat{\phi}_{z}^{\Sigma pu} \\ \hline \boldsymbol{\phi}_{\boldsymbol{dq}}^{\boldsymbol{\Delta}pu} \end{bmatrix} = \begin{bmatrix} \hat{C}_{\sigma}^{pu} \boldsymbol{v}_{\boldsymbol{Cdq}}^{\boldsymbol{\Sigma}pu} \\ \hat{C}_{\sigma z}^{pu} \hat{v}_{Cz}^{\Sigma pu} \\ \hline \hat{C}_{\sigma}^{pu} \boldsymbol{v}_{\boldsymbol{CdqZ}}^{\boldsymbol{\Delta}pu} \\ \hline \hat{L}_{\sigma}^{pu} \boldsymbol{i}_{\boldsymbol{dq}}^{\boldsymbol{\Sigma}pu} \\ \hat{L}_{\sigma z}^{pu} \hat{i}_{z}^{\Sigma pu} \\ \hline \hat{L}_{\delta}^{pu} \boldsymbol{i}_{\boldsymbol{dq}}^{\boldsymbol{\Delta}pu} \end{bmatrix} \tag{15}$$

In addition, the control vector $\boldsymbol{u}$ is now expressed as:

$$\boldsymbol{u} = \begin{bmatrix} \boldsymbol{m}_{\boldsymbol{dq}}^{\boldsymbol{\Sigma}\top} & \hat{m}_{z}^{\Sigma} \mid \boldsymbol{m}_{\boldsymbol{dq}}^{\boldsymbol{\Delta}\top} \end{bmatrix}^{\top} \tag{16}$$

The energy stored in the system; or what is the same, the Hamiltonian function has still the structure given in (3) yet with $\boldsymbol{x}$ defined as in (15) and Q as in (17a), with $\boldsymbol{Q^C}$ and $\boldsymbol{Q^L}$ the upper and lower diagonal sub-matrices respectively defined in (17b) and (17c).

$$\boldsymbol{Q} = \begin{bmatrix} \boldsymbol{Q}_{7\times7}^{\boldsymbol{C}} & \boldsymbol{0}_{7\times5} \\ \hline \boldsymbol{0}_{5\times7} & \boldsymbol{Q}_{5\times5}^{\boldsymbol{L}} \end{bmatrix} \tag{17a}$$

$$\boldsymbol{Q^C} = \mathrm{diag}(\hat{C}_{\sigma}^{pu-1}, \hat{C}_{\sigma}^{pu-1}, \hat{C}_{\sigma z}^{pu-1}, \underbrace{\hat{C}_{\sigma}^{pu-1}, ..., \hat{C}_{\sigma}^{pu-1}}_{1\times4}) \tag{17b}$$

$$\boldsymbol{Q^L} = \mathrm{diag}(\hat{L}_{\sigma}^{pu}, \hat{L}_{\sigma}^{pu}, \hat{L}_{\sigma z}^{pu}, \hat{L}_{\delta}^{pu}, \hat{L}_{\delta}^{pu}) \tag{17c}$$

Furthermore, the gradient of the Hamiltonian function $\boldsymbol{\nabla H(x)}$ is obtained by taking the partial derivatives of $H(\boldsymbol{x})$ with respect to each of the state variables, resulting in (18). As indicated by the second equality in (18), $\boldsymbol{\nabla H(x)}$ represents the voltage and current vectors in the new per unit representation.

$$\begin{aligned} \boldsymbol{\nabla} H\left(\boldsymbol{x}\right) &= \begin{bmatrix} \frac{\boldsymbol{q}_{\boldsymbol{Cdq}}^{\boldsymbol{\Sigma}pu\top}}{\hat{C}_{\sigma}^{pu}} & \frac{\hat{q}_{Cz}^{\Sigma pu}}{\hat{C}_{\sigma z}^{pu}} \mid \frac{\boldsymbol{q}_{\boldsymbol{CdqZ}}^{\boldsymbol{\Delta}pu\top}}{\hat{C}_{\sigma}^{pu}} \mid \frac{\boldsymbol{\phi}_{\boldsymbol{dq}}^{\boldsymbol{\Sigma}pu\top}}{\hat{L}_{\sigma}^{pu}} & \frac{\hat{\phi}_{z}^{\Sigma pu}}{\hat{L}_{\sigma z}^{pu}} \mid \frac{\boldsymbol{\phi}_{\boldsymbol{dq}}^{\boldsymbol{\Delta}pu\top}}{\hat{L}_{\delta}^{pu}} \end{bmatrix}^{\top} \\ &= \begin{bmatrix} \boldsymbol{v}_{\boldsymbol{Cdq}}^{\boldsymbol{\Sigma}pu\top} & \hat{v}_{Cz}^{\Sigma pu} \mid \boldsymbol{v}_{\boldsymbol{CdqZ}}^{\boldsymbol{\Delta}pu\top} \mid \boldsymbol{i}_{\boldsymbol{dq}}^{\boldsymbol{\Sigma}pu\top} & \hat{i}_{z}^{\Sigma pu} \mid \boldsymbol{i}_{\boldsymbol{dq}}^{\boldsymbol{\Delta}pu\top} \end{bmatrix}^{\top} \end{aligned} \tag{18}$$

The vector $\boldsymbol{E}$ representing the sources of the converter is now defined using per unit representation as in (19), where $\boldsymbol{v}_{\boldsymbol{dq}}^{\boldsymbol{G}pu} = \boldsymbol{v}_{\boldsymbol{dq}}^{\boldsymbol{G}}/V_B$ and $v_{dc,pu} = v_{dc}/V_{Bdc}$.

$$\boldsymbol{E} = \omega_b 2 \begin{bmatrix} \boldsymbol{0}_{1\times9} & v_{dc,pu} & -v_{d,pu}^{G} & -v_{q,pu}^{G} \end{bmatrix}^{\top} \tag{19}$$

The matrix that is being multiplied by the gradient of the Hamiltonian represented by $(\boldsymbol{J}_0 + \sum_{i=1}^{m} \boldsymbol{J}_i u_i - \boldsymbol{R})$ is given in (20) for the system with the proposed modifications. From this matrix it is possible to first extract the dissipation matrix $\boldsymbol{R}$ as given in (21).

$$\boldsymbol{R} = \omega_b \begin{bmatrix} \boldsymbol{0}_{7\times7} & \boldsymbol{0}_{7\times5} \\ \hline \boldsymbol{0}_{5\times7} & \begin{matrix} \hat{R}_{\sigma}^{pu} & 0 & 0 & 0 \\ 0 & \hat{R}_{\sigma}^{pu} & 0 & 0 & 0 \\ 0 & 0 & \hat{R}_{\sigma z}^{pu} & 0 & 0 \\ 0 & 0 & 0 & \hat{R}_{\delta}^{pu} & 0 \\ 0 & 0 & 0 & 0 & \hat{R}_{\delta}^{pu} \end{matrix} \end{bmatrix} \tag{21}$$

Similarly, the interconnection matrix $\boldsymbol{J}_0$ can also be extracted from (20), yielding in a similar structure as in (12) yet with the sub-matrices $\boldsymbol{J}_0^C$ and $\boldsymbol{J}_0^L$ defined as in (22).

$$\boldsymbol{J}_0^C = \omega \begin{bmatrix} 0 & 2\hat{C}_{\sigma}^{pu} & 0 & 0 & 0 & 0 & 0 \\ -2\hat{C}_{\sigma}^{pu} & 0 & 0 & 0 & 0 & 0 & 0 \\ 0 & 0 & 0 & 0 & 0 & 0 & 0 \\ 0 & 0 & 0 & 0 & \hat{C}_{\sigma}^{pu} & 0 & 0 \\ 0 & 0 & 0 & -\hat{C}_{\sigma}^{pu} & 0 & 0 & 0 \\ 0 & 0 & 0 & 0 & 0 & 0 & 3\hat{C}_{\sigma}^{pu} \\ 0 & 0 & 0 & 0 & 0 & -3\hat{C}_{\sigma}^{pu} & 0 \end{bmatrix} \tag{22a}$$

$$\boldsymbol{J}_0^L = \omega \begin{bmatrix} 0 & 2\hat{L}_{\sigma}^{pu} & 0 & 0 & 0 \\ -2\hat{L}_{\sigma}^{pu} & 0 & 0 & 0 & 0 \\ 0 & 0 & 0 & 0 & 0 \\ 0 & 0 & 0 & 0 & \hat{L}_{\delta}^{pu} \\ 0 & 0 & 0 & -\hat{L}_{\delta}^{pu} & 0 \end{bmatrix} \tag{22b}$$

Notice that here too $\boldsymbol{J}_0$ is skew-symmetric as $\boldsymbol{J}_0^C = -\boldsymbol{J}_0^{C\top}$ and $\boldsymbol{J}_0^L = -\boldsymbol{J}_0^{L\top}$.

Finally, all the $m = 5$ control related interconnection matrices $\boldsymbol{J}_i$ under the proposed variable change are here extracted from (20). Each of these matrices can be represented as in (13a), where the internal submatrices are given in (23). Notice that under the proposed variable change, $\boldsymbol{J}_i^C = -\boldsymbol{J}_i^L$ for $i = 1, ..., 5$, implying that skew-symmetry is achieved for all the interconnection matrices.

$$\omega_b \overbrace{\begin{bmatrix} 0 & 0 & 1 & 0 & 0 \\ 0 & 0 & 0 & 0 & 0 \\ 1 & 0 & 0 & 0 & 0 \\ 0 & 0 & 0 & 1 & 0 \\ 0 & 0 & 0 & 0 & -1 \\ 0 & 0 & 0 & 1 & 0 \\ 0 & 0 & 0 & 0 & 1 \end{bmatrix}}^{\boldsymbol{J}_1^C}; \; \omega_b \overbrace{\begin{bmatrix} 0 & 0 & -1 & 0 & 0 & 0 & 0 \\ 0 & 0 & 0 & 0 & 0 & 0 & 0 \\ -1 & 0 & 0 & 0 & 0 & 0 & 0 \\ 0 & 0 & 0 & -1 & 0 & -1 & 0 \\ 0 & 0 & 0 & 0 & 1 & 0 & -1 \end{bmatrix}}^{\boldsymbol{J}_1^L} \tag{23a}$$

$$\left(\boldsymbol{J}_0 + \sum_{i=1}^{m} \boldsymbol{J}_i \boldsymbol{u}_i - \boldsymbol{R}\right) = \ldots \tag{20}$$

$$\omega_b \left[\begin{array}{ccccccc|ccccc}
0 & \hat{C}_\sigma^{pu} 2\omega_{pu} & 0 & 0 & 0 & 0 & 0 & \hat{m}_z^\Sigma & 0 & m_d^\Sigma & m_d^\Delta & -m_q^\Delta \\
-\hat{C}_\sigma^{pu} 2\omega_{pu} & 0 & 0 & 0 & 0 & 0 & 0 & 0 & \hat{m}_z^\Sigma & m_q^\Sigma & m_q^\Delta & m_d^\Delta \\
0 & 0 & 0 & 0 & 0 & 0 & 0 & m_d^\Sigma & m_q^\Sigma & \frac{\hat{m}_z^\Sigma}{2} & m_d^\Delta & m_q^\Delta \\
0 & 0 & 0 & 0 & \hat{C}_\sigma^{pu} \omega_{pu} & 0 & 0 & m_d^\Delta & m_q^\Delta & m_d^\Delta & m_d^\Sigma + \hat{m}_z^\Sigma & m_q^\Sigma \\
0 & 0 & 0 & -\hat{C}_\sigma^{pu} \omega_{pu} & 0 & 0 & 0 & -m_q^\Delta & m_d^\Delta & m_q^\Delta & m_q^\Sigma & \hat{m}_z^\Sigma - m_d^\Sigma \\
0 & 0 & 0 & 0 & 0 & 0 & \hat{C}_\sigma^{pu} 3\omega_{pu} & m_d^\Delta & -m_q^\Delta & 0 & m_d^\Sigma & -m_q^\Sigma \\
0 & 0 & 0 & 0 & 0 & -\hat{C}_\sigma^{pu} 3\omega_{pu} & 0 & m_q^\Delta & m_d^\Delta & 0 & m_q^\Sigma & m_d^\Sigma \\
\hline
-\hat{m}_z^\Sigma & 0 & -m_d^\Sigma & -m_d^\Delta & m_q^\Delta & -m_d^\Delta & -m_q^\Delta & -\hat{R}_\sigma^{pu} & \hat{L}_\sigma^{pu} 2\omega_{pu} & 0 & 0 & 0 \\
0 & -\hat{m}_z^\Sigma & -m_q^\Sigma & -m_q^\Delta & -m_d^\Delta & m_q^\Delta & -m_d^\Delta & -\hat{L}_\sigma^{pu} 2\omega_{pu} & -\hat{R}_\sigma^{pu} & 0 & 0 & 0 \\
-m_d^\Sigma & -m_q^\Sigma & -\frac{\hat{m}_z^\Sigma}{2} & -m_d^\Delta & -m_q^\Delta & 0 & 0 & 0 & 0 & -\hat{R}_{\sigma z}^{pu} & 0 & 0 \\
-m_d^\Delta & -m_q^\Delta & -m_d^\Delta & -m_d^\Sigma - \hat{m}_z^\Sigma & -m_q^\Sigma & -m_d^\Sigma & -m_q^\Sigma & 0 & 0 & 0 & -\hat{R}_\delta^{pu} & \hat{L}_\delta^{pu} \omega_{pu} \\
m_q^\Delta & -m_d^\Delta & -m_q^\Delta & -m_q^\Sigma & m_d^\Sigma - \hat{m}_z^\Sigma & m_q^\Sigma & -m_d^\Sigma & 0 & 0 & 0 & -\hat{L}_\delta^{pu} \omega_{pu} & -\hat{R}_\delta^{pu}
\end{array}\right]$$

$$\omega_b \overbrace{\begin{bmatrix} 0&0&0&0&0 \\ 0&0&1&0&0 \\ 0&1&0&0&0 \\ 0&0&0&0&1 \\ 0&0&0&1&0 \\ 0&0&0&0&-1 \\ 0&0&0&1&0 \end{bmatrix}}^{\boldsymbol{J}_2^C}; \; \omega_b \overbrace{\begin{bmatrix} 0&0&0&0&0&0&0 \\ 0&0&-1&0&0&0&0 \\ 0&-1&0&0&0&0&0 \\ 0&0&0&0&-1&0&-1 \\ 0&0&0&-1&0&1&0 \end{bmatrix}}^{\boldsymbol{J}_2^L} \tag{23b}$$

$$\omega_b \overbrace{\begin{bmatrix} 1&0&0&0&0 \\ 0&1&0&0&0 \\ 0&0&1/2&0&0 \\ 0&0&0&1&0 \\ 0&0&0&0&1 \\ 0&0&0&0&0 \\ 0&0&0&0&0 \end{bmatrix}}^{\boldsymbol{J}_3^C}; \; \omega_b \overbrace{\begin{bmatrix} -1&0&0&0&0&0&0 \\ 0&-1&0&0&0&0&0 \\ 0&0&-1/2&0&0&0&0 \\ 0&0&0&-1&0&0&0 \\ 0&0&0&0&-1&0&0 \end{bmatrix}}^{\boldsymbol{J}_3^L} \tag{23c}$$

$$\omega_b \overbrace{\begin{bmatrix} 0&0&0&1&0 \\ 0&0&0&0&1 \\ 0&0&0&1&0 \\ 1&0&1&0&0 \\ 0&1&0&0&0 \\ 1&0&0&0&0 \\ 0&1&0&0&0 \end{bmatrix}}^{\boldsymbol{J}_4^C}; \; \omega_b \overbrace{\begin{bmatrix} 0&0&0&-1&0&-1&0 \\ 0&0&0&0&-1&0&-1 \\ 0&0&0&-1&0&0&0 \\ -1&0&-1&0&0&0&0 \\ 0&-1&0&0&0&0&0 \end{bmatrix}}^{\boldsymbol{J}_4^L} \tag{23d}$$

$$\omega_b \overbrace{\begin{bmatrix} 0&0&0&0&-1 \\ 0&0&0&1&0 \\ 0&0&0&0&1 \\ 0&1&0&0&0 \\ -1&0&1&0&0 \\ 0&-1&0&0&0 \\ 1&0&0&0&0 \end{bmatrix}}^{\boldsymbol{J}_5^C}; \; \omega_b \overbrace{\begin{bmatrix} 0&0&0&0&1&0&-1 \\ 0&0&0&-1&0&1&0 \\ 0&0&0&0&-1&0&0 \\ 0&-1&0&0&0&0&0 \\ 1&0&-1&0&0&0&0 \end{bmatrix}}^{\boldsymbol{J}_5^L} \tag{23e}$$

V. Model validation via time-domain simulations

To validate the port-Hamiltonian modelling approach including the proposed variable changes, results from time-domain simulation of the following three different models will be shown and discussed in this section.

1) The port-Hamiltonian SSTI Model: including the proposed variable changes discussed in section IV and represented by the equations (15)-(20), considered to be the main contribution of this paper. Simulations result obtained with this model are identified in the legend by a $\star$ symbol as a superscript for each variable.

2) The SSTI MMC model proposed in [8]: used as the starting point for the derivations of the port-Hamiltonian representation. This modelling approach was briefly recalled in section II-C and its derivation is based on Fig. 2. This model will be identified in the legend by "REF".

TABLE II. NOMINAL VALUES & PARAMETERS

U_{1n}	380[kV]	R_f	0.3429[Ω]	k_{i_Δ}	21.4000
f_n	50[Hz]	L_f	62.92[mH]	k_{i_Σ}	21.8750
v_{dc}	775.67[kV]	R_σ	0.6017[Ω]	$k_{p\Sigma}$	1.1141
C_σ	21.1619[μF]	L_σ	30.64[mH]	$k_{p\Delta}$	2.6010

3) The AAM of a three-phase MMC: where each arm is represented by a controlled voltage source and where the internal arm voltage dynamics is represented by an equivalent arm capacitance as indicated in the lower right part of Fig. 1 [9], [10], [11]. This model includes non-linear effects except for the switching operations and the dynamics of the sub-module capacitor voltage balancing algorithm, as discussed in 2. Since this model is well-established for analysis and simulation of MMCs and has been previously verified in comparison to experimental results [9], [10], it will be used as a benchmark reference for verifying both the validity of port-hamiltonain MMC model, as well as the SSTI of [8]. Simulation results obtained with this model are identified in the legend by "AAM".

The models are all simulated in Matlab/Simulink with the SimPowerSystem toolbox. Furthermore, all simulations are based on the MMC HVDC single-terminal configuration shown in 1, with the parameters given in Table II under the well known Circulating Current Suppression Control (CCSC) technique described in [22] and standard SRRF vector control for the grid current, similarly to what was presented in [8], and shown in Fig. 3. For comparing the models, it should be considered that the "AAM" model is a conventional time-domain simulation model of a three-phase MMC, while the SSTI model from [8] ("REF") as well as the port-Hamiltonian formulation here presented both represent the MMC dynamics by variables transformed into a set of SRRFs. Nonetheless, comparison of transient and steady-state response is simpler when the variables have SSTI representation. Thus, in most cases, the results obtained from the reference model are transformed into the appropriate SRRFs to ease the comparison. However, the results from the SSTI models can also be transformed to the stationary phase coordinates, although this would imply comparison of signals with sinusoidal or multi-frequency oscillations in steady-state. All results are plotted in per unit quantities. To excite the MMC dynamics in the different models, the ac-side active power reference is reduced from 0.62 *p.u.* to -0.62 *p.u.* at $t = 0.02s$.

The dynamics of the voltage sum $\boldsymbol{v^{\Sigma}_{Cdqz}}$ for the above described case scenario are illustrated in Fig. 4. More precisely, the dq components of the voltage sum are given in the upper plot, while the zero-sequence is given

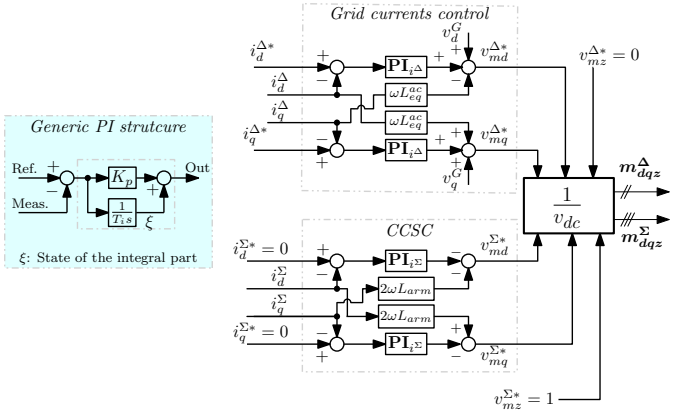

Fig. 3. Circulating Current Suppression Control (CCSC) and standard SRRF grid current vector control

in the lower one. From Fig. 4, it can be seen how the variables calculated with the AAM-MMC as well as the REF model are overlapping those calculated with the port-Hamiltonian model derived in this paper. This is true both under transient and steady-state conditions.
Notice that the steady-state value of v^{Σ}_{Cz} changes with respect to each of the reference steps, as only the CCSC is implemented assuming no regulation of the capacitive energy stored in the MMC. Furthermore, the non-zero steady-state values of $\boldsymbol{v^{\Sigma}_{Cdq}}$ reflect the 2ω oscillations that this variable has in the stationary abc reference frame.

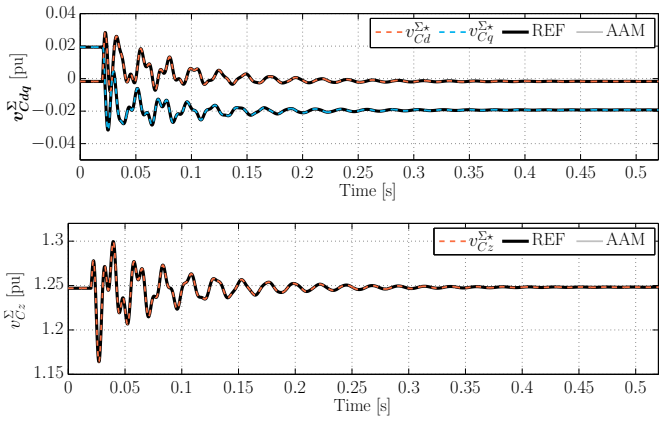

Fig. 4. Voltage sum

Similarly, the dynamics of the energy difference $\boldsymbol{v^{\Delta}_{Cdqz}}$ are depicted in Fig. 5. More precisely, the upper figure is illustrating the dq components behaviour of this variable under the above described case scenario while the lower figure does the same for the zero-sequence. In terms of accuracy, both of the sub-figures show how the proposed port-Hamiltonian modelling approach with the proposed changes accurately captures the behaviour of

both the SSTI MMC model of [8] as well as the AAM-MMC model. Notice that the comparison associated

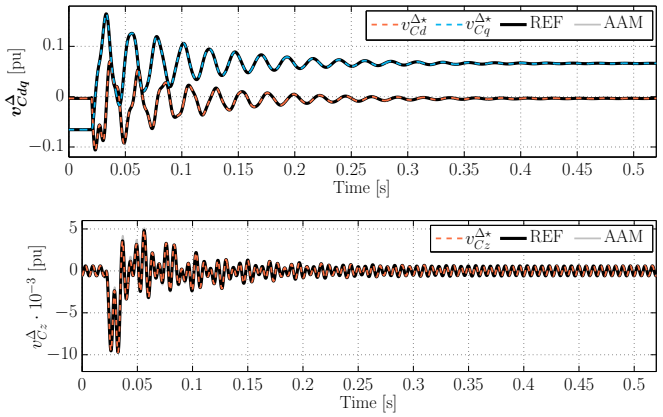

Fig. 5. Voltage difference

to v_{Cz}^{Δ} has been done in a SSTP framework, instead of its equivalent SSTI version $\boldsymbol{v}_{\boldsymbol{CZ}}^{\boldsymbol{\Delta}}$ [8]. This is done for simplicity, as the dynamics of the virtual system used to create $\boldsymbol{v}_{\boldsymbol{CZ}}^{\boldsymbol{\Delta}}$ do not directly exist in the AAM-MMC model. However, for the sake of completeness, the dynamics of $\boldsymbol{v}_{\boldsymbol{CZ}}^{\boldsymbol{\Delta}}$ obtained with the derived port-Hamiltonian representation, as well as with the SSTI model of [8] are depicted in Fig. 6, where it can be confirmed that both the $v_{CZ_d}^{\Delta}$ and $v_{CZ_q}^{\Delta}$ sub-variables reach a constant value in steady-state operation.

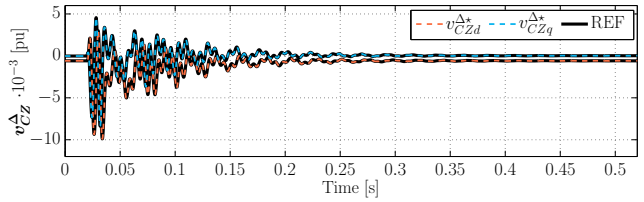

Fig. 6. Voltage difference with constant equilibrium point

The dynamics of the circulating currents $\boldsymbol{i}_{\boldsymbol{dqz}}^{\boldsymbol{\Sigma}}$ are shown in Fig. 7, where the upper sub-figure depicts the dynamics of the dq components while the lower figure shows the zero-sequence components. From the figure it can be also concluded that the derived port-Hamiltonian representation of the MMC including the proposed change of variables accurately replicates the dynamic behaviour of the reference model.

Finally, the dynamics of the dq components of the grid current are shown in Fig. 8. It is possible to see that for this variable the reference SSTI model, the AAM and the derived port-Hamiltonian representation of the MMC are practically overlapping.

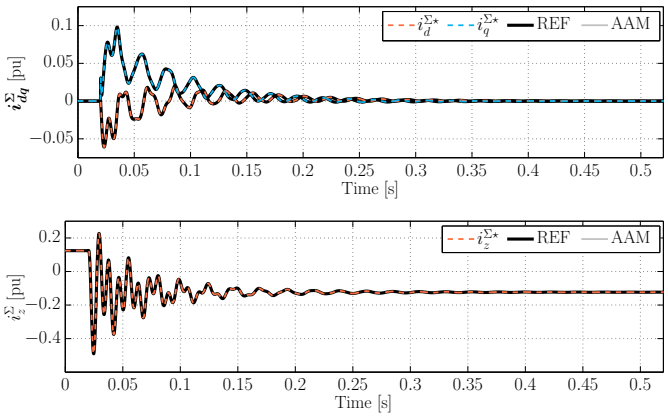

Fig. 7. Circulating current

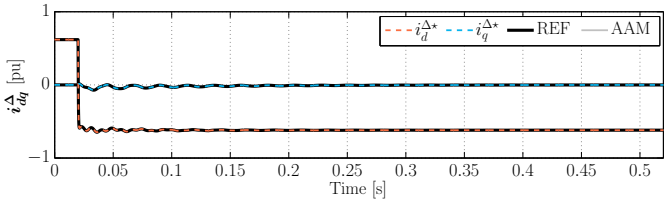

Fig. 8. Grid current

VI. Conclusion

This paper presents a reformulation of the state-space representation of the averaged model of the Modular Multilevel Converter (MMC) such that it is suitable for the generalized Hamiltonian formalism. The port-Hamiltonian modelling approach provides a natural starting point for non-linear control design methods, such as Passivity-based control techniques, aiming to design globally asymptotically stable controllers. Furthermore, it usually requires a dynamic system representation of the system under study with constant variables in steady-state; i.e., with an equilibrium point as opposed to an equilibrium orbit. Unfortunately, the well-established continuous MMC model able to capture the averaged dynamics of the converter and widely used for control design, has oscillatory variables in steady-state and is not suited for the intended mathematical formalism. Therefore, this study is based on the recently proposed steady-state time-invariant (SSTI) model of the MMC, which is able to replicate the averaged dynamics of the converter while preserving its non-linear structure.

An attempt to directly formulate the SSTI MMC model in a port-Hamiltonian framework is first carried out to identify the limitations of the SSTI MMC model for this application. It was found that the interconnection matrices associated to the control did not comply with the required skew-symmetry property of the mathemat-

ical formalism under consideration. Therefore, several variable changes were proposed, including a per-unit notation system, in order to reformulate the system into an equivalent one with skew-symmetric interconnection matrices. Finally, this equivalent model is expressed under the port-Hamiltonian framework and validated via time-domain simulations with respect to both the SSTI MMC model used as a starting point for the derivation, as well as with the well-established averaged model of the converter.

AKNOWLEDGEMENTS

The authors would like to thank Jon Are Suul from SINTEF Energy, as well as Julian Freytes from L2EP-Ecole Centrale de Lille, for their help and support in making this work possible.

REFERENCES

[1] B. M. Maschke, A. J. van der Schaft, and P. C. Breedveld, "An intrinsic hamiltonian formulation of the dynamics of lc-circuits," *IEEE Transactions on Circuits and Systems I: Fundamental Theory and Applications*, vol. 42, no. 2, pp. 73–82, Feb 1995.

[2] A. van der Schaft and B. Maschke, "The hamiltonian formulation of energy conserving physical systems with external ports," *AEU. Archiv für Elektronik und Übertragungstechnik*, vol. 49, no. 5-6, pp. 362–371, 1995.

[3] G. Escobar, A. J. Van Der Schaft, and R. Ortega, "A hamiltonian viewpoint in the modeling of switching power converters," *Automatica*, vol. 35, no. 3, pp. 445–452, 1999.

[4] V. Duindam, A. Macchelli, S. Stramigioli, and H. Bruyninckx, *Modeling and control of complex physical systems: the port-Hamiltonian approach*. Springer Science & Business Media, 2009.

[5] A. van der Schaft and D. Jeltsema, "Port-hamiltonian systems theory: An introductory overview," *Foundations and Trends in Systems and Control*, vol. 1, no. 2-3, pp. 173–378, 2014.

[6] H. K. Khalil and J. Grizzle, *Nonlinear systems*. Prentice hall New Jersey, 1996, vol. 3.

[7] M. Hernandez-Gomez, R. Ortega, F. Lamnabhi-Lagarrigue, and G. Escobar, "Adaptive pi stabilization of switched power converters," *IEEE Transactions on Control Systems Technology*, vol. 18, no. 3, pp. 688–698, May 2010.

[8] G. Bergna, J. A. Suul, and S. D'Arco, "State-space modelling of modular multilevel converters for constant variables in steady-state," in *2016 IEEE 17th Workshop on Control and Modeling for Power Electronics (COMPEL)*, June 2016, pp. 1–9.

[9] L. Harnefors, A. Antonopoulos, S. Norrga, L. Angquist, and H.-P. Nee, "Dynamic analysis of modular multilevel converters," *Industrial Electronics, IEEE Transactions on*, vol. 60, no. 7, pp. 2526–2537, July 2013.

[10] S. Rohner, J. Weber, and S. Bernet, "Continuous model of modular multilevel converter with experimental verification," in *2011 IEEE Energy Conversion Congress and Exposition*, Sept 2011, pp. 4021–4028.

[11] A. Christe and D. Duji, "State-space modeling of modular multilevel converters including line frequency transformer," in *Power Electronics and Applications (EPE'15 ECCE-Europe), 2015 17th European Conference on*, Sept 2015, pp. 1–10.

[12] A. Antonopoulos, L. Angquist, and H. P. Nee, "On dynamics and voltage control of the modular multilevel converter," in *2009 13th European Conference on Power Electronics and Applications*, Sept 2009, pp. 1–10.

[13] K. Ilves, A. Antonopoulos, S. Norrga, and H.-P. Nee, "Steady-state analysis of interaction between harmonic components of arm and line quantities of modular multilevel converters," *IEEE Transactions on Power Electronics*, vol. 27, no. 1, pp. 57–68, January 2012.

[14] R. H. Park, "Two-reaction theory of synchronous machines:; generalized method of analysis - part i," *AIEE Transactions*, vol. 48, pp. 716–730, July 1929.

[15] J. Beerten, S. D'Arco, and J. A. Suul, "Identification and small-signal analysis of interaction modes in vsc mtdc systems," *IEEE Transactions on Power Delivery*, vol. 31, no. 2, pp. 888–897, April 2016.

[16] A. a. J. Far and D. Jovcic, "Circulating current suppression control dynamics and impact on mmc converter dynamics," in *2015 IEEE Eindhoven PowerTech*, June 2015, pp. 1–6.

[17] A. Jamshidifar and D. Jovcic, "Small-signal dynamic dq model of modular multilevel converter for system studies," *IEEE Transactions on Power Delivery*, vol. 31, no. 1, pp. 191–199, Feb 2016.

[18] V. Najmi, M. N. Nazir, and R. Burgos, "A new modeling approach for modular multilevel converter (mmc) in d-q frame," in *2015 IEEE Applied Power Electronics Conference and Exposition (APEC)*, March 2015, pp. 2710–2717.

[19] T. Li, A. M. Gole, and C. Zhao, "Harmonic instability in mmc-hvdc converters resulting from internal dynamics," *IEEE Transactions on Power Delivery*, vol. 31, no. 4, pp. 1738–1747, Aug 2016.

[20] P. Kundur, *Power System Stability and Control*. New York, USA: McGraw-Hill, 1994.

[21] Q. Tu, Z. Xu, and J. Zhang, "Circulating current suppressing controller in modular multilevel converter," in *IECON 2010 - 36th Annual Conference on IEEE Industrial Electronics Society*, Nov 2010, pp. 3198–3202.

[22] Q. Tu, Z. Xu, and L. Xu, "Reduced switching-frequency modulation and circulating current suppression for modular multilevel converters," in *Transmission and Distribution Conference and Exposition (T D), 2012 IEEE PES*, May 2012, pp. 1–1.